VOL. 15, NO. 23, DECEMBER 2020 ISSN 1819-6608
ARPN Journal of Engineering and Applied Sciences

www.arpnjournals.com

SEDIMENTARY CHARACTERISTICS, XRD, FTIR, UV-Vis AND ROCK-EVAL PYROLYSIS OF BLACK SHALE INTERVALS OF THE SEMANTAN FORMATION, PENINSULAR MALAYSIA

Zulqarnain Sajid[1], Mohd. Suhaili Ismail[1], Tanzila Hanif[2], Haylay Tsegab[1], Shahid Ali[2] and Nisar Ahmed[1]
[1]Department of Petroleum Geosciences, Universiti Teknologi Petronas (UTP), Sri Iskandar, Malaysia
[2]Institute of Geology, University of the Punjab, Lahore, Pakistan
E-Mail: zulqarnainsajid786@gmail.com

ABSTARCT

This study provides a systematic characterization of Triassic turbidites associated black shale of the Semantan Formation, extensively distributed in the NS part of the Central Belt, Peninsular Malaysia. Sedimentary characteristics, XRD, FTIR, UV-Vis, and Rock-Eval pyrolysis analysis of the black shale from four different localities were studied. XRD analysis shows that illite and kaolinite are dominant clay minerals with abundant traces of non-clay mineral such as quartz. FTIR spectra indicate the presence of aromatic carbon, aromatic C-H in plane bending, and aromatic C-H out of plane bending, OH functional group within black shale organic matter, and traces of quartz. TOC contents are highly variable (0.2-3.67, average: 1.37 wt %) and sourced from allochthonous organic material. The rock-Eval analysis shows that the black shale of the Semantan Formation comprises Type-III kerogens, which propose organic input from terrestrial high plants. UV-Vis absorption ratios E2/E4 (A254/A436) are also used to distinguish between the terrestrial and autochthonous sources of organic matter.

Keywords: Semantan formation, turbidities, organic matter, Peninsular Malaysia.

1. INTRODUCTION

Turbidities associated deposits of Semantan Formation are geologically and geographically most significant in the NS part of the Central Belt of Peninsular Malaysia. Since the 1980s, there is a huge increasing impact of turbidites associated deposits on worldwide petroleum reserves. Mostly hydrocarbon associated resources from deep-marine have been known from Cenozoic-age. At the same time, there is an ambiguous but increasing contribution from reservoirs of older age rocks as well such as Triassic-Jurassic and Cretaceous ages. About 90% of these resources are discovered from turbidites associated sandstone reservoirs [1]. Turbidites associated black shale in the petroleum system play an important role as a source and seal rock in many offshore and onshore sedimentary basins worldwide. In the last few decades, many efforts have been made by various researchers to develop a better understanding of the type of organic matter, quality, maturation, and generation of organic matter in these host rocks by utilizing organic geochemical identities.

Although Triassic turbidites associated deposits of the Semantan Formation are extensively distributed in the Central Belt of Peninsular, the mineralogy and organic geochemical characteristics, particular their black shales sequences, have not been investigated before. In this paper, XRD, UV-Vis, FTIR, and Rock-Eval pyrolysis characteristics of black shales have been analysed. XRD, UV-Vis, and FTIR were utilized to determine the type of hydrocarbon functional groups, mineral material, and source of organic influx. Further, Rock-Eval pyrolysis is used to interpret the kind of organic matter, maturation, and kerogen types. However, until now, not much literature available about the nature of organic matter, the functional groups, and mineral matter present within the black shales. For the study, a total of six black shale samples for XRD, four samples for FTIR, UV-Vis, and Rock-Eval Pyrolysis analysis were collected from four sections and analyzed.

2. GEOLOGICAL SETTING

Black shales of the Semantan Formation are extensively distributed in the NS part of Central Belt of Peninsular Malaysia (Figures-1and 2). During the Triassic times, the East Malaya/Indo-china plates collided with Sibumasu block and formed a suture zone known as Bentong-Raub Suture [2]. During this period, many sedimentary basins created on structural highs due to intense deformation. Afterward, such basins became the depositional sites for the deep-marine turbidite deposits.

VOL. 15, NO. 23, DECEMBER 2020 ISSN 1819-6608
ARPN Journal of Engineering and Applied Sciences

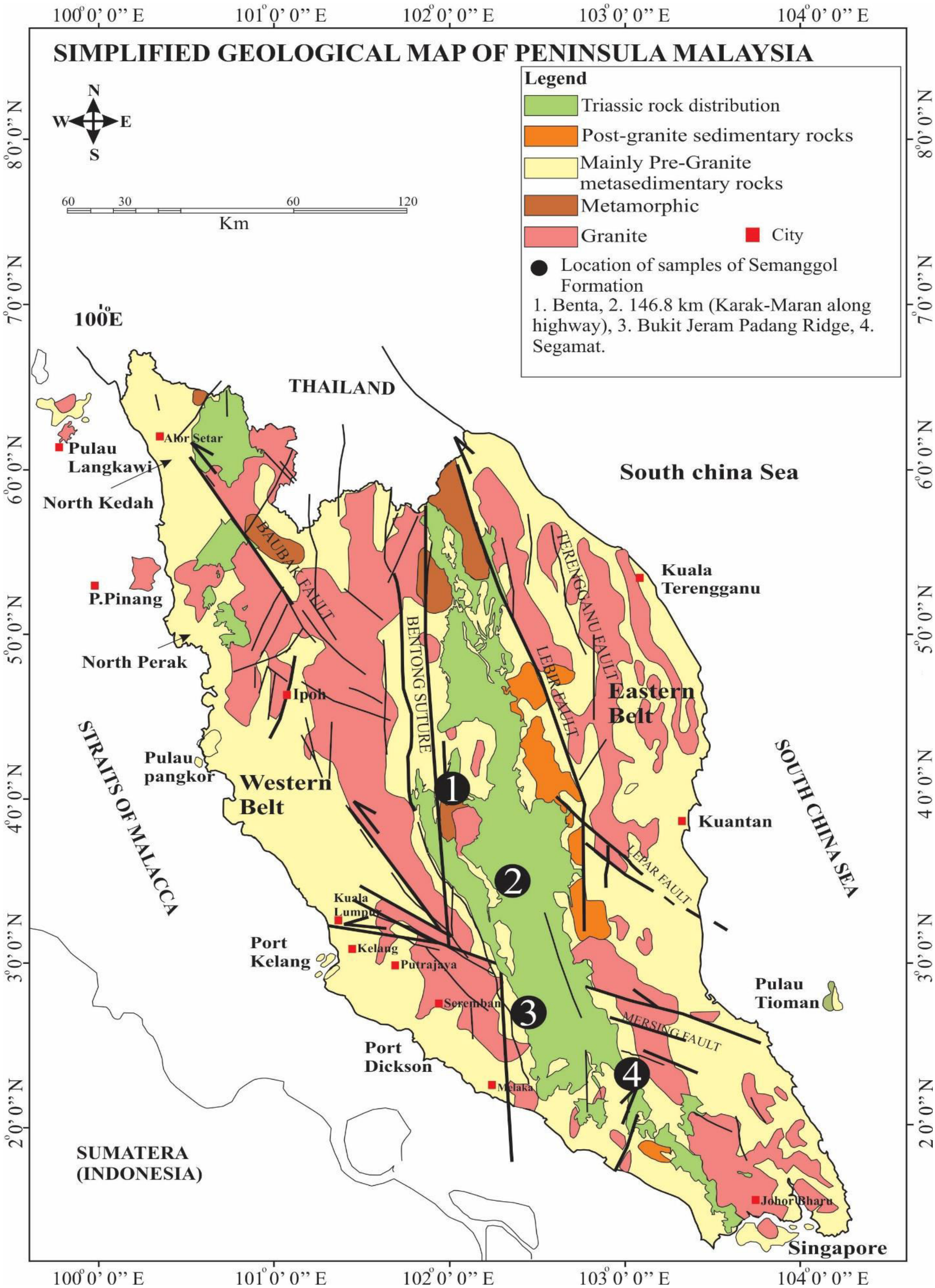

Figure-1. Geological map illustrating the field localities of measured stratigraphic sections from the Semantan Formation [3].

VOL. 15, NO. 23, DECEMBER 2020 ISSN 1819-6608
ARPN Journal of Engineering and Applied Sciences

www.arpnjournals.com

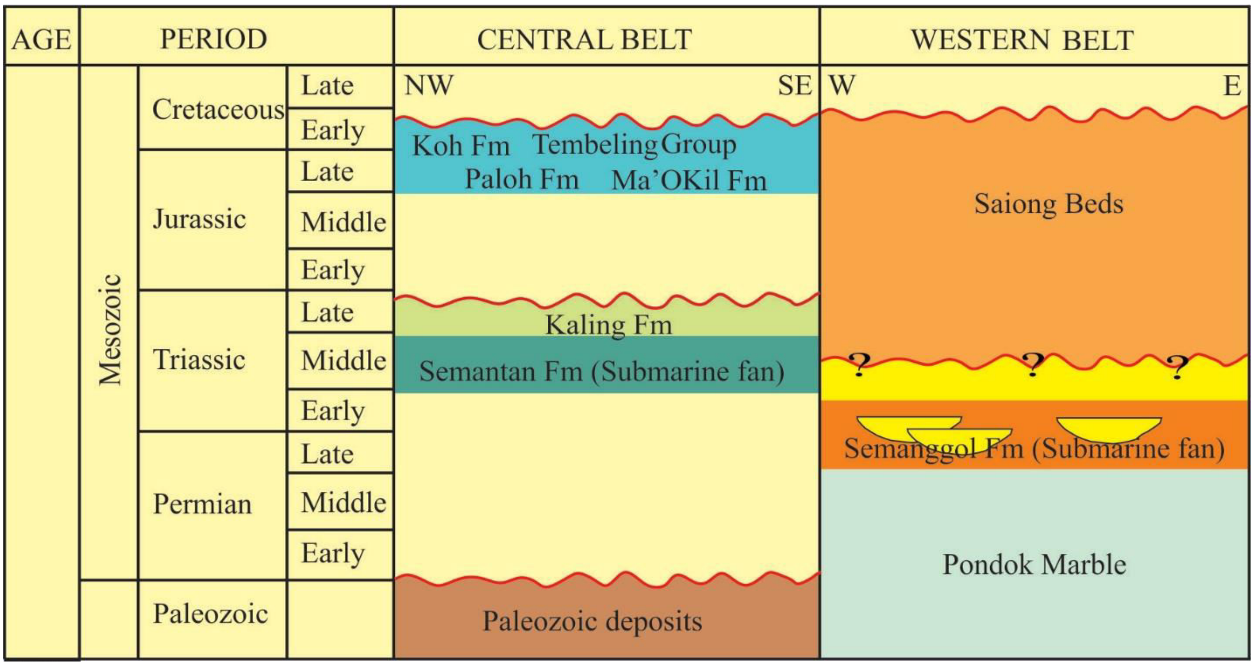

Figure-2. Stratigraphic distribution of Triassic rocks in the West Belt and Central Belt, Peninsular Malaysia [4].

Ahmad [5] named the exposures of rocks at Sungai Semantan as Semantan Formation in the Karak-Temerloh area. Due to rapid subsidence and basin margin instability, the formation became intensely folded and faulted. Therefore, the estimation of Semantan Formation's real thickness is much challenging, but more than 2 km thick succession recorded along highways of Karak-Temerloh and Mantakab-Temerloh [6]. Towards the south, these sedimentary sequences approximated to be more than 4.3 km thick [7]. The outcrops of the Semantan Formation have extended from Karak to Maran and from north to west Johor in Central Belt of Peninsular Malaysia [8] (Figures-1 and 2). The Semantan Formation has unconformable upper contact with Lanis Conglomerate and Mangking Sandstone of Jurassic-Cretaceous age in Karak to Maran areas, and with the Maokil and Paloh formations in the Johor area [4]. The Semantan Formation is highly fossiliferous locally but mostly barren and dominant in two main lithologies, i.e., shale and tuffaceous siltstone [6]. The Semantan Basin was predominated by flysch-type sediments and associated rhyolitic/andesitic volcanism, volcanoclastics, interbedded carbonaceous shale, and argillaceous sandstone suggesting that the Semantan Basin was a foreland/ rift margin or graben basin formed in response to collisional tectonics [9].

3. MATERIALS AND METHODS

3.1Collection of Samples

Six samples from four different localities have been collected for detailed studies such as 1-Benta section, 2-146.8 km section (Karak-Maran highway section), 3-Bukit Jeram Padang Ridge section, and 4-Segamat section. The sample details in respect of lithology, depth, geological age, and location are shown in Figure-3.

3.2 Stratigraphic Logging

To prepare the field-based stratigraphic log, information have been collected by using Jacob staff, measuring tape, geological hammer, hand-lens, and 10% dilute Hydrochloric acid. All the information while making the stratigraphic log noted on graphically notepad, keeping in mind the standard procedure explained by Tucker [10]. The prime purpose of the field stratigraphic log is to simplify the outcrop geology and made it more understandable to recognize the stratigraphic setup. Basically, outcrop logging based on the observation of physical exposures of different rock units. Particularly for the sedimentary facies, data about physical nature of contact-relationship of different sedimentary rocks, grain size, color (fresh and weathering color), texture, and fossil contents was collected from the outcrops.

3.3 TOC and Rock-Eval Pyrolysis

Before selecting the samples for Rock-Eval pyrolysis, TOC contents of these were determined at the Department of Petroleum Geosciences, Universiti Teknologi PETRONAS, Malaysia, by using a Source Rock Analyzer (SRA-Weatherford). After that, about 10mg of each sample were sent to CGG professional Laboratory, Aberdeen, the United Kingdom for Rock-Eval pyrolysis.

3.4 Acid Treatment to Remove Inorganic Carbon

Black shale samples were pulverized into a fine powder and treated the powder sample with 50 ml of 37% concentrated hydrochloric acid then placed the solution on hot-plate at temperature of 60 °C until completion of reaction. The solution was washed with distilled water three times and dried overnight in an oven at 60 °C to completely remove the carbonates before any further analysis.

3.4.1 Fourier Transform Infrared spectrometry (FTIR) analysis

According to the standard procedure of Painter *et al.* [11], pellets of 1mg of crushed samples were prepared, which were grounded up to the size of 75mm with 100mg KBr for the FTIR analysis. The data was collected by using a Cary 660 Series FTIR Spectrometer equipped with PIKE MIRACLE diamond attenuated total reflectance spectroscopy (ATR). FTIR pattern of the black shale samples was determined in absorbance mode at 4000 cm^{-1} to 450 cm^{-1} wavelength resolution. The detection limit of the analysis is 0.08%.

3.4.2 Ultraviolet-visible (UV-Vis) spectroscopy

The primary focus of this study is to note the ratios of E2/E3, E2/E4, E3/E4, and E4/E6 to determine the aromaticity, humification, and source of organic matter. The humic matter was enhanced and then extracted by the U.S. EPA method 3550 using ultrasonic extraction with Methanol used as a solvent. Two grams of each sample placed in capped bottles. The sample treated three times with 8 mL of methanol to the extracted humic substance by stirring it three minutes each time and further five minutes stirring by centrifugation at 2500 rpm. The instrument used for the UV–VIS was Perkineler lambda 750 UV-Vis spectrophotometer. The UV-Vis spectra for the black shale samples were determined between 200-800 nm wavelength range.

3.5 X-ray diffraction (XRD) of black shale

The mineralogical composition of black shale is determined by X-ray diffraction (XRD). For XRD analysis, both bulk and clay fractions of the black shale were used. Bulk rock samples were pulverized by agate mortar and placed in the X-ray frame. The clay fractions of black shale were separated by placing 10g of the sample in 600ml beaker and added dilute 1 M acetic acid to remove carbonates. After some time, when there is no reaction in solution, the residue was washed with distilled water.

Further, the removal of organic matter content was done by treating the samples with 30% concentrated hydrogen peroxide (H_2O_2). Complete disaggregated rock samples were gone through several washes with distilled water to suspend all clay particles. Suspended clay fractions were sucked by dropper and placed on glass slides and left for dry. Three slides prepared for every four samples as (i) one for untreated, (ii) second slide treated with ethylene glycol vapor at 60°C for 1 hour, and (iii) the third slide heated at 550°C for 3 hours. Both bulk shale samples and clay fractions were analysed by utilizing the Bruker D8 X-ray generator with Ni–filtered Cu–Kα, operated at 40kV and 25mA. For the bulk samples, scans showed a limited range between 2 and 80°2θ clay fractions varied from 2 to 40°2θ. The analysis performed at the Department of Petroleum Geosciences, Universiti Teknologi PETRONAS, Malaysia.

4. RESULTS

To study the turbidites associated deposits in detail at field, different parameters like lithology, grain size, sedimentary structures, and geometry of different rock beds carefully examined because these features give deep insight for interpreting the depositional settings. The whole study area dominantly covered by deep-marine turbidites associated deposits, i.e., conglomerate, sandstone, black shale, and volcanoclastic rock facies along with mass transport deposits.

The Semantan Formation stratigraphic sections were measured from Benta, 146.8 km (Karak-Maran highway) Pahang, Bukit Jeram Padang Ridge, and Segamat, Johor, Central Belt (Figure-1). Six major lithofacies have been identified in these stratigraphic sections such as 1-Conglomerate, 2-Pebbly sandstone, 3-Thick bedded sandstone, 4-Interbedded sandstone and shale heterolith, 5-Black shale/or black mudstone and 6-Slump dominant lithofacies (Figure-3). Turbidities associated black shale of the Semantan Formation is thick to medium bedded, dark grey to black having top contact with volcanoclastic sediments in most of the sections. In contrast, lower contact is with thin alternate bedding of sandstone-siltstone and shale, which is further overlain by conglomerate dominated facies (Figure-4).

ISSN 1819-6608
ARPN Journal of Engineering and Applied Sciences

www.arpnjournals.com

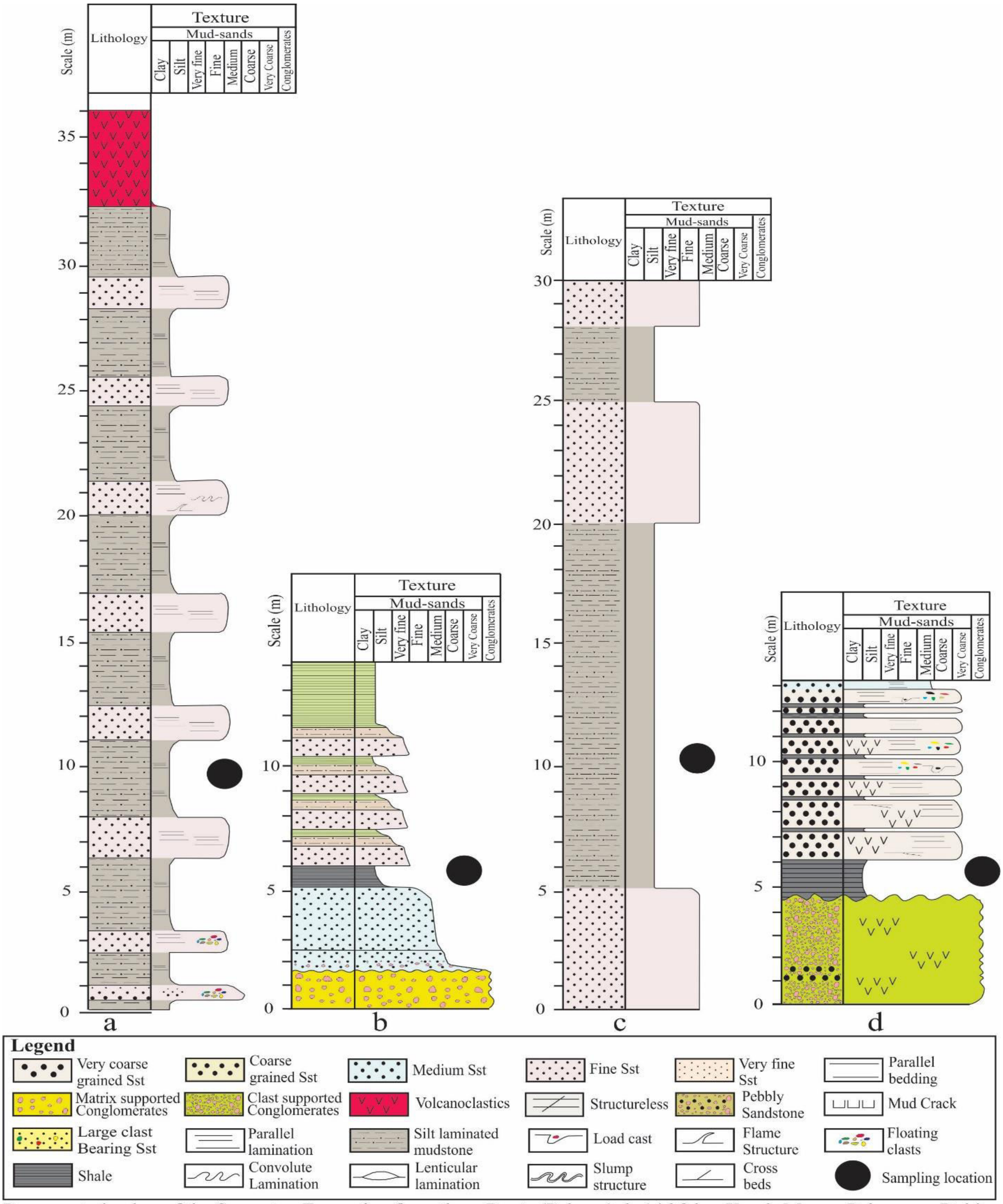

Representative log of the Semantan Formation from the a-Benta (Pahang); b-146.8 km Karak-Maran, Pahang; c- Bukit Jeram Padang ridge(Johor) and d-Segamat (Johor), Peninsular Malaysia.

Figure-3. Stratigraphic sections from four different locations of the Semantan Formation, Peninsular Malaysia.

VOL. 15, NO. 23, DECEMBER 2020 ISSN 1819-6608
ARPN Journal of Engineering and Applied Sciences

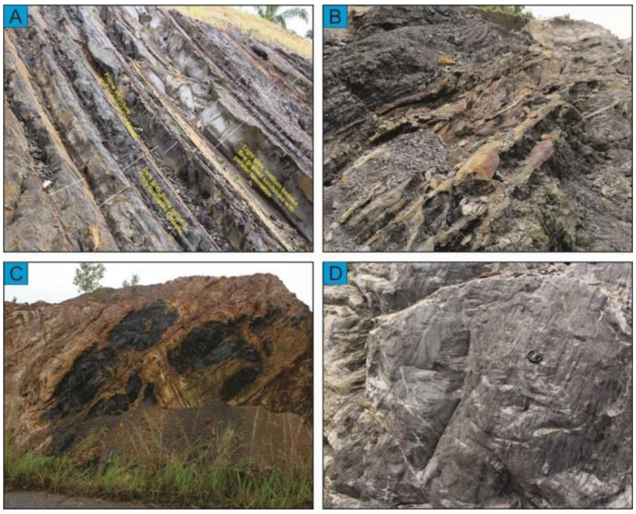

Figure-4. Black shale lithofacies of the Semantan Formation from the a-Benta (Pahang); b-146.8 km Karak-Maran, Pahang; c- Bukit Jeram Padang ridge (Johor) and d-Segamat (Johor), Peninsular Malaysia.

4.1 Rock-Eval Pyrolysis

TOC along with Rock-Eval pyrolysis for the four samples are shown in Table-1. The total organic carbon content range from 0.58 wt.% to 11.69 wt. % (average: 4.23 wt.%), but a sample from Segamat section shows exceptionally high TOC content having a value of 11.69 wt.% suggesting the formation is fair to excellent source rock. The cross-plot of S2 versus TOC reveals the similar results (Figure-5A). The plot of TOC versus S1 (Figure-5B) can be utilized to distinguish among non-indigenous hydrocarbons (allochthonous) and indigenous hydrocarbons (autochthonous). This plot indicates that the majority of the studied black shale samples characterized as allochthonous hydrocarbons representing that the source rock itself did not produce the organic matter. The hydrocarbon generation potential (PY = S1 + S2) varies from poor to good for black shale of the Semantan Formation (Figure-5C). The production index (PI) values range between 0.25 and 0.50 (average: 0.32). In the diagram of Tmax vs. PI, three samples fall in the inert carbon field and one sample in the migrated hydrocarbon field (Figure-5D).

Table-1. Rock-Eval pyrolysis results of the black shales of Semantan Formation.

Section Name	TOC (wt. %)	Tmax (°C)	S1 (mg HC / g rock)	S2 (mg HC / g rock)	S3 (mg CO_2/g rock)	HI (mg HC / g rock)	OI(mg CO_2/g rock)	PI (S1/S1+S2)	PY (S1+S2)
Benta	1.00	367	20	20	120	2	12	0.50	40
146.8 Km Karak-Maran section	3.67	608	50	120	220	3	6	0.29	170
Bukit Jeram Padang ridge	0.58	501	10	30	110	5	19	0.25	40
Segamat	11.69	610	20	60	910	1	8	0.25	80

 ISSN 1819-6608
ARPN Journal of Engineering and Applied Sciences

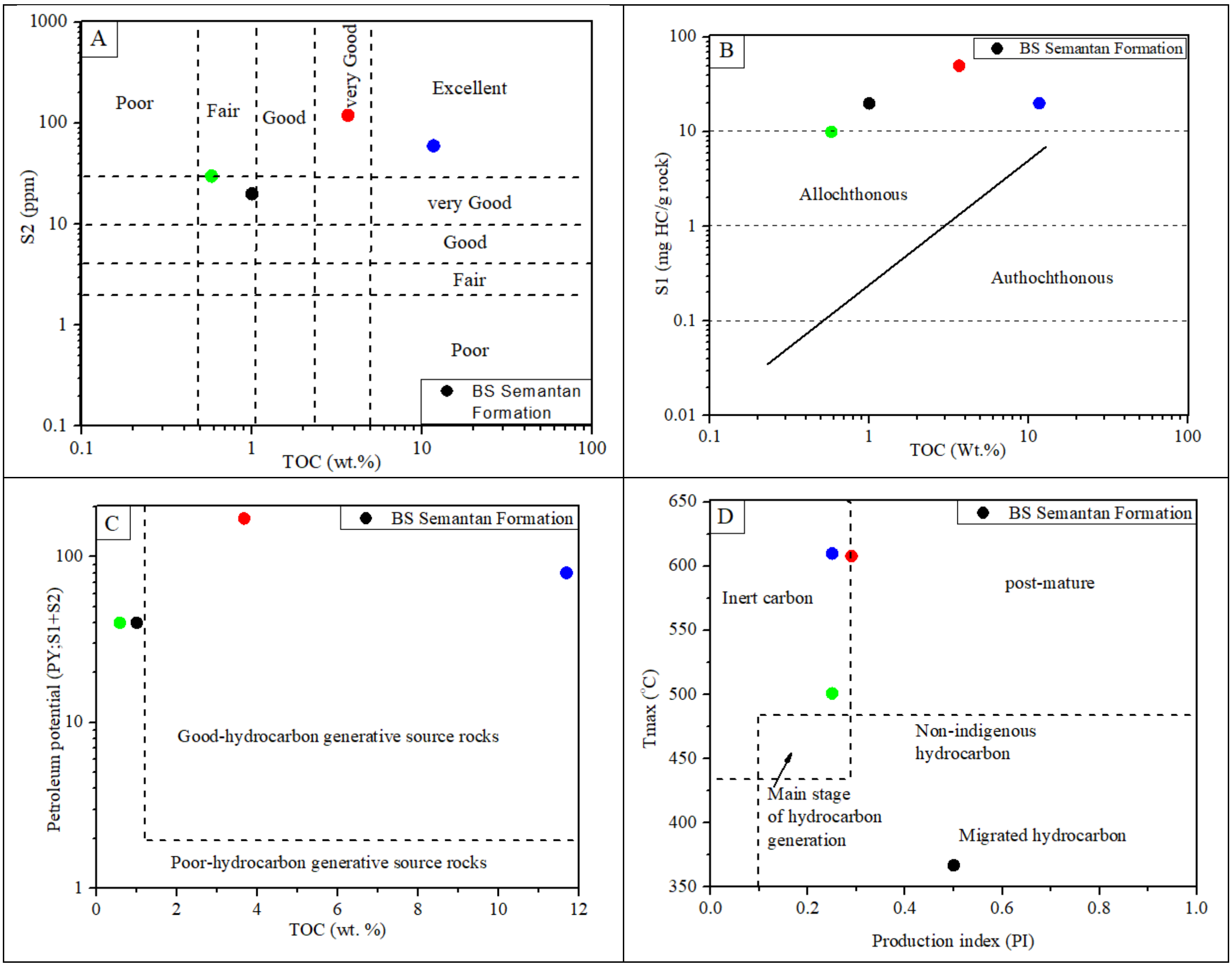

Figure-5. A) Binary plot of S2 versus TOC (wt.%), B) Plot of TOC vs S1 used to distinguish between non-indigenous (allochthonous) and indigenous hydrocarbons (autochthonous) [12], C) Illustrating the relationship between hydrocarbon generation and TOC (wt. %) [12], D) Cross-plot of Tmax pyrolysis versus production index.

The hydrogen index (HI) of the 4 selected samples range between 1 and 5 mg/(g of TOC) (average: 2.75 mg/(g of TOC)) and oxygen index (OI) vary from 6 to 19 mg/(g of TOC) (average: 11.25 mg/(g of TOC)) (Table-1). Plots of TOC vs S2 (Figure-6A) and Tmax against HI (Figure-6B) represent that black shale samples show their trend towards type-III kerogen. The Tmax values vary from 367 to 610°C for all samples, indicating post–mature thermal evolution.

 ISSN 1819-6608
ARPN Journal of Engineering and Applied Sciences

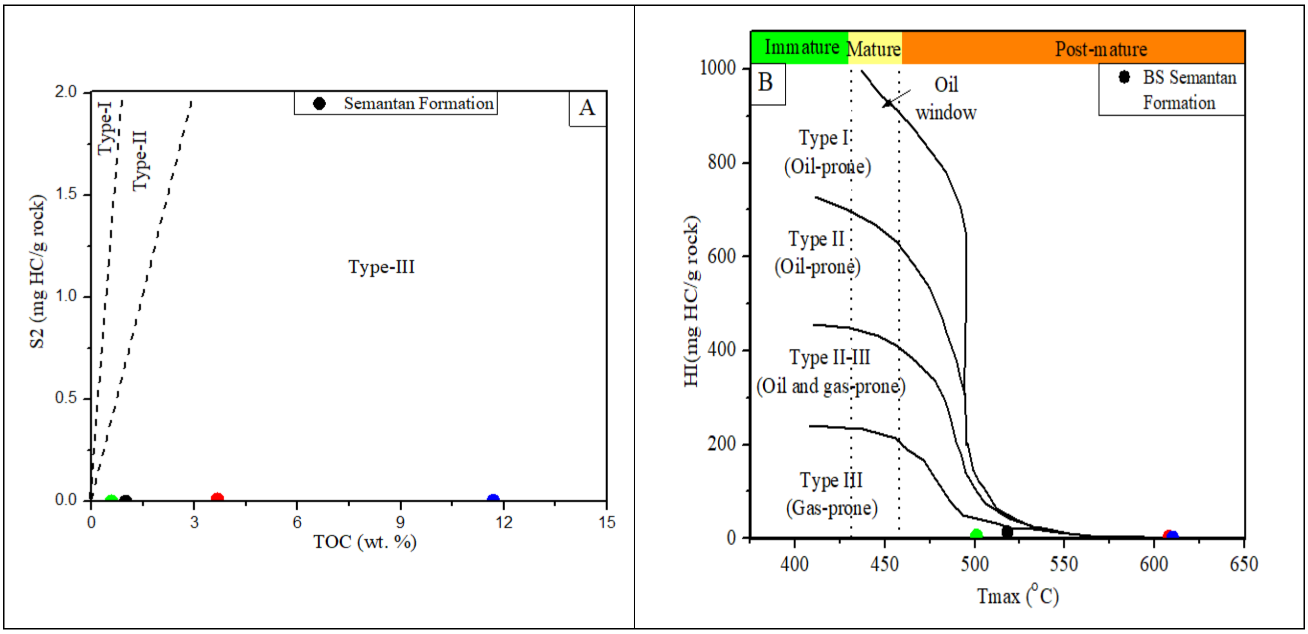

Figure-6. A) Plot of S2 versus TOC [13], B) Plot of T_{max} vs Hydrogen Index (HI) is showing generative source rock potential for the Triassic turbidites black shales from Peninsular Malaysia [14].

4.2 Mineralogy

XRD results are shown in Figure-7 (A and B) for clay fractions of the Semantan Formation. Kaolinite and illite are the only clay minerals that interpreted in the XRD spectrum for the studied black shale. Illite diffraction peaks can be noted at d=~9.79 Å and 4.9 Å. The X-ray diffraction spectral of the Semantan illite correlates well with that of the pure illite (d=10.1, 5.00, and 3.38 Å). In contrast, kaolinite diffraction peaks identified at d=~7.06 Å and 3.54, 3.55 Å. Non–clay minerals noticed, i.e., predominantly quartz grains. Therefore, the XRD pattern of black shale revealed that illite, kaolinite, and quartz were significant constituents of Semantan shale.

ARPN Journal of Engineering and Applied Sciences

www.arpnjournals.com

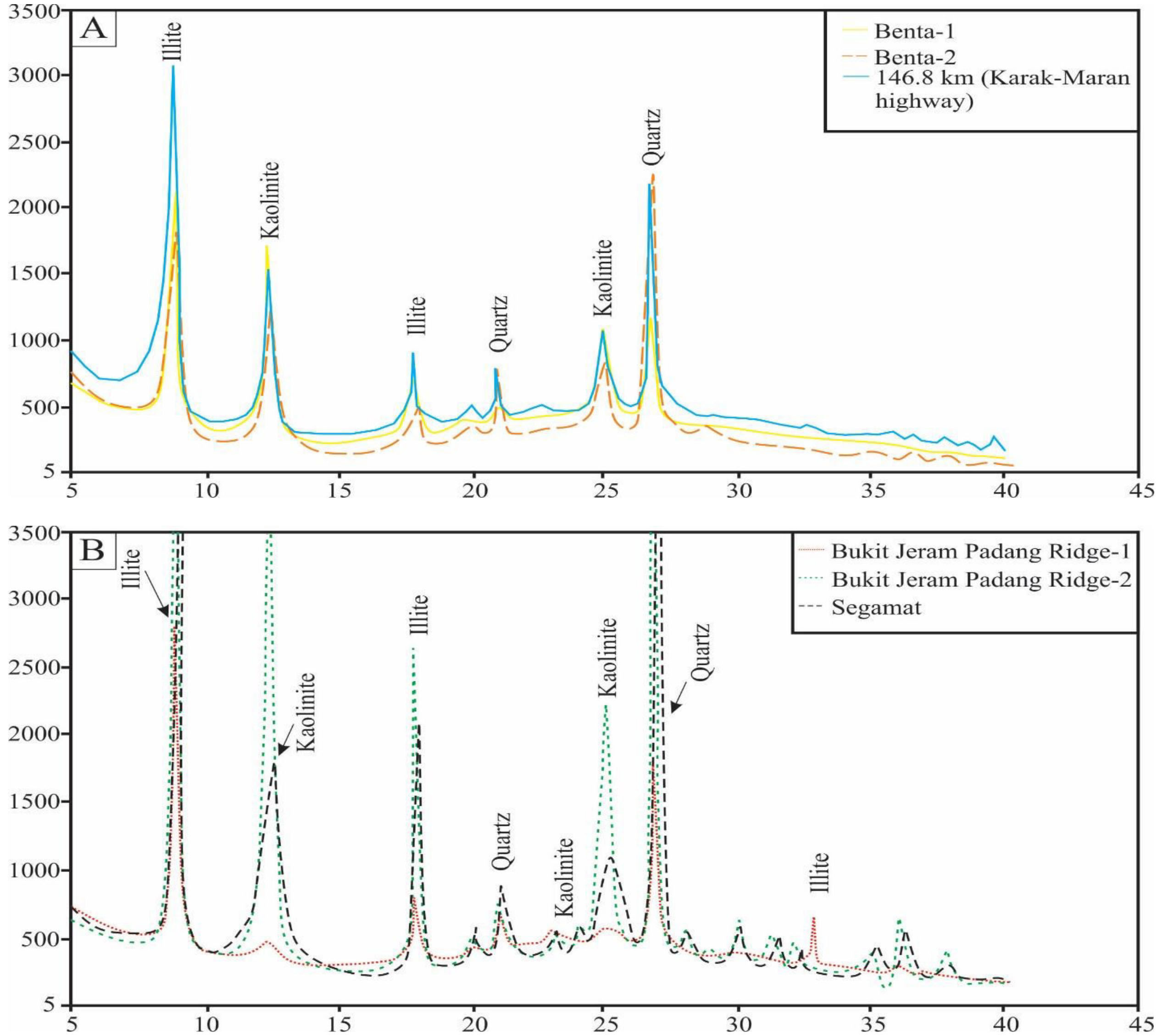

Figure-7. A, B) X-ray diffraction pattern of the clay fraction separated from the black shale of the Semantan Formation.

4.3 Fourier Transform Infrared Spectroscopy (FTIR)

Table-2 shows the different functional groups of hydrocarbon identified in the black shale samples through FTIR analysis. Among the Semantan black shales, aromatic C=C stretching is observed between 1621 cm^{-1} to 1624 cm^{-1}. Aromatic in Plane C-H bending and Aromatic out of Plane C-H bending is identified between 1031 cm^{-1} to 1166.2 cm^{-1} and 630 cm^{-1} to 9.14 cm^{-1}, respectively. Further, OH stretching vibration is observed at 3393 cm^{-1} to 3698 cm^{-1} (Figure-8).

VOL. 15, NO. 23, DECEMBER 2020 ISSN 1819-6608
ARPN Journal of Engineering and Applied Sciences

www.arpnjournals.com

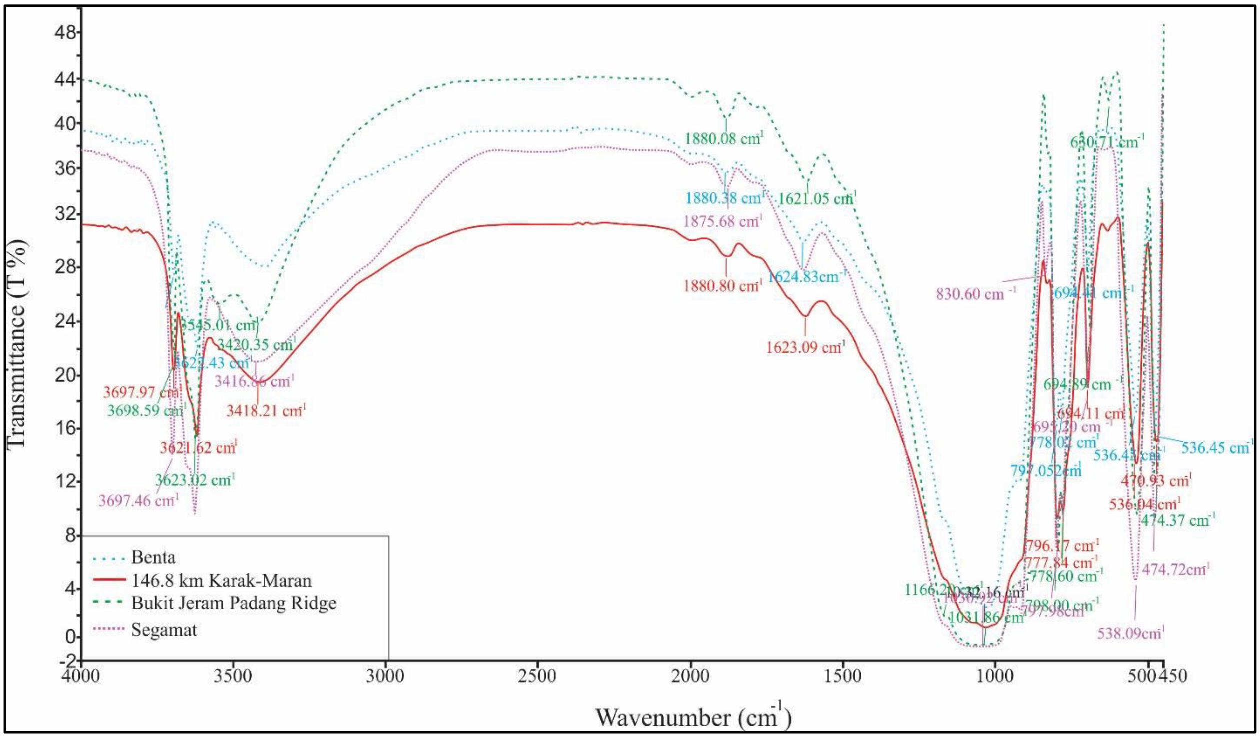

Figure-8. FTIR spectra of black shale of the Semantan Formation.

Table-2. Functional groups identified by FTIR spectra of the Semantan Blak shale.

Section	Transmittance	Absorbance	Wavenumber (cm^{-1})					
			Free –OH 3393-3698 stretching	**Aromatic overtone and combination bands**	**Aromatic C=C 1621-1624 stretching**	**Aromatic In-Plane C-H bending 1031- 1166**	**Aromatic 630-914 C-H out-of-plane bending**	**C-X stretching (X=F, Cl, Br or I)/P-Br stretching/P-S stretching**
Benta	15.54-21.85	0.56-0.81	3420.35-3698.59					
	39.7	0.40		1880.08				
	35.02	0.46			1621.05			
	0.62-2.74	1.56-2.21				1031.86-1166.2		
	7.23-40.89	0.39-1.14					630.71-798	
	9.96-12.76	0.89-1.00						474.37-537.07
146.8 Km Karak-Maran section	35.49	0.45		1875				
	29.09	0.54						
	3.06-28.65	0.54-1.51					695.2-914.05	
	5.33-9.78	1.01-1.27						474.72-538.09
	10.33-22.15	0.65-0.99	3416.86-3697.46					
Bukit Jeram Padang ridge	22.08-28.31	0.55-0.66	3393.81-3697.75					
	30.35	0.52			1624.83			
	35.63	0.45		1881.38				
	15.46-27.23	0.56-0.81					694.41-797.52	
	15.15-16.91	0.77-0.82						536.45-472.92
Segamat	15.36-20.38	0.69-0.81	3418.21-3697.97					
	28.94	0.54		1880.8				
	24.43	0.61			1623.09			
	1.06	1.97				1032.16		
	9.16	1.04					694.11-796.17	
	18.88-9.83	0.72-1.01						
	14.75	0.83						53.04-470.93

4.4. Ultraviolet-Visible Spectroscopy (UV-Vis)

Ultraviolet-visible spectroscopy spectra obtained by adopting standard procedure explained by Cunha et al. [15] between 200 to 800 nm wavelength. Different ratios of E2/E3, E2/E4, E3/E4, and E4/E6 were used to determine the aromaticity, humification, and source of organic matter (Table-3). Ratios of E2/E3 and E2/E4 have been utilized to indicate the aromaticity of dissolved organic matter (DOM) [16]. The degree of humification is one of the critical parameters that can be derived from absorption ratios of E4/E6 (A465/A665). Besides the ratios already discussed above, absorption ratios of E2/E4 has been used to differentiate between the relative composition of autochthonous and terrestrial DOM [17]. Absorption ratios at wavenumber A465 and A665 are not identified in all analysed samples.

ARPN Journal of Engineering and Applied Sciences

Table-3. UV-Vis absorption ratios of four samples of the Semantan black shale treated with methanol.

Type	Absorption ratio	Benta	146.8 Km	Bukit Jeram Padang ridge	Segamat	Range	Source	Relationship	Reference
		Absorption ratios							
E2/E4	A254/A436	3.36	6.56	5.99	4.95	(4.37-11.34)[1]	River	Estimate the relative composition of autochthonous versus terrestrial DOM	[1]Battin [18]
E3/E4	A340/A254	0.40	0.27	0.26	0.28	(0.20-0.38)[2]	River	To predict DOC concentration	[2]Tipping et al. [19]
E2/E3	A250/A365	3.32	5.36	5.60	4.76	(4.16-5.72)[3]	River, lake water humic substances	Negatively correlate with aromaticity and MW	[3]Peuravuori and Pihlaja [20]
E2/E3	A254/A365	3.19	5.29	4.40	4.40	(3.5-10.7)[4]	Plant or manure DOM	Negatively correlate with aromaticity and MW	[4]Hunt and Ohno [21]
E3/E4	A300/A400	2.33	3.66	3.34	2.60	(3.4-8.4)[5]	Lake	Negatively correlate with humification	[5]Erlandsson et al. [22]

5. DISCUSSIONS

5.1 Depositional History

During the Mesozoic Era, a significant part of the newly-formed landmass of the Peninsula was elevated and persisted in being exposed sub-aerially. Marine sedimentation was centred in two depocenters named as northwestern Kodiang-Semanggol and Gua Musang-Semantan depocenters in the Central Belt. The Gua Musang-Semantan depocentre was extended over a vast area and was formed on the shelf of East Malaya of Upper Paleozoic. During Triassic times, in the Gua Musang-Semantan depocentre, the widespread distributions of tuff and associated lava, tuffaceous siliciclastic, and conglomerate are indicative of active volcanic activities and basinal instability that prevailed during Basin's life span. In the deeper parts of the Gua Musang-Semantan depocentre, thick turbidite accumulations have been deposited. During late Triassic time, a new regional pattern of sedimentation was developed as a result of tectonic disturbances and extensive plutonism that resulted in the formation of Main Range, Central Belt, and Eastern Belt plutons. Voluminous sediments, eroding from newly uplifted sources, were transported and infilled existing basins [4]. During the Middle Triassic times due to segmentation and intensified subsidence of Gua Musang-Semantan Basin, sea level gradually deepened towards the western side, and the depositional environment shifted from oxic to anoxic in the deep parts of the basin, establishing favorable conditions for organic matter accumulation. The eastern side of the Semantan Basin was dominated by shallow water facies like rudite-arenites, which were deposited in a high-energy environment as regression progressed during the last stage of the Indosinian Orogeny and deposition took place in the oxic water column [4] [23].

A total of six lithofacies identified which further characterized into four facies association and represents different parts of the submarine fan system from proximal to distal. However, black shales represent the deposition in the distal part of the submarine fan system characterized by thin-thick bedding with parallel lamination.

5.2 XRD, Rock-Eval Pyrolysis UV-Vis and FTIR

XRD analysis of the black shales of the Semantan Formation reveals that the dominant clay-mineral identified is illite and kaolinite with traces of non-clay minerals such as quartz. Illite crystallinity index values vary from 0.50 to 0.58° $\Delta 2\theta$, with an average of 0.53° $\Delta 2\theta$. These values suggest deep-marine diagenetic conditions for the formation of these clay minerals.

TOC, along with Rock-Eval pyrolysis for the four samples suggesting the black shale of Semantan Formation is fair to good source rock. The plot of TOC versus S1 characterized the hydrocarbon as allochthonous, representing that the source rock itself did not produce the organic matter. The hydrocarbon generation potential (PY = S1 + S2) varies from poor to good for black shale of the Semantan Formation. Further cross-plot of Tmax vs. PI, represents the majority of the samples represent inert carbon field, and one sample shows its trend towards the migrated hydrocarbon field. Dembicki [24] reported that allochthonous organic matter is the product of terrestrial higher plants contributing biomass to the fluvial system that carries this organic matter from the river mouth to the deep marine setting by turbidity currents.

Based on UV-Vis absorption ratios of E2/E3, E2/E4, and E3/E4, it is suggested that the source of organic matter is terrestrial and negatively correlate with humification and aromaticity. The negative correlation of TOC with different absorption ratios shows that there is no relationship between these two parameters (Figure-9A).

VOL. 15, NO. 23, DECEMBER 2020 ISSN 1819-6608
ARPN Journal of Engineering and Applied Sciences

www.arpnjournals.com

Furthermore, the concentration of TOC is inversely related to absorption ratios, such as TOC increased absorption ratios decreased likely (Figure-9B).

The dominance of aromatic compounds has been seen in the FTIR spectra of Semantan black shale samples (Figure-8). Aromatic in-plane C-H bending peaks are identified at 1031.86, 1032, 1166.2, and aromatic C-H out of plane bending peaks at 630.71, 695.2, 794.11, 796.14, 797.52, 798, 914.05. Si-O and Al-O peaks at 474.37, 474.72, 472.92, and 536.45, 537.07, 538.09 respectively. Aromatic C=C stretching peaks observed at 1621.05, 1623.09, 1624.83 and aromatic overtone and combination bands peaks at 1875, 1880.08, 1880.8, and 1881.38. OH functional group peaks observed at 3393.81, 3416.86, 3418.21, 3420.35, , 3697.46, 3697.75, 3697.97, 3698.59.

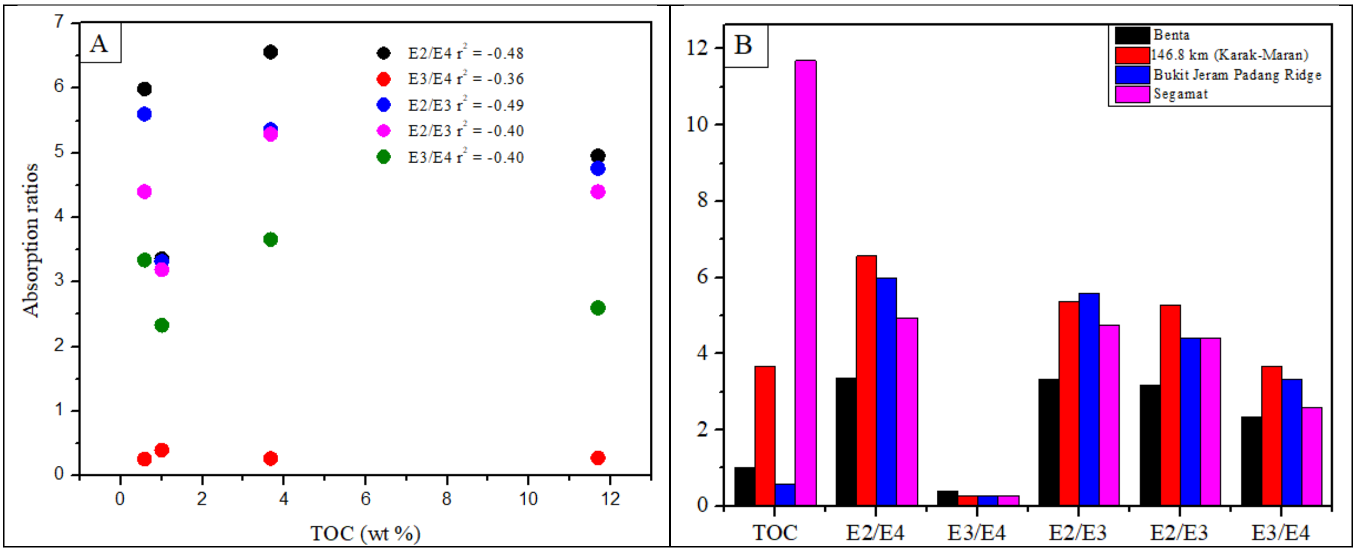

Figure-9. A) Cross Plot of TOC vs UV-Vis absorption ratios, and B) Concentrations of TOC and UV-Vis absorption ratio from Benta, 146.8 km (Karak-Maran), Bukit Jeram Padang Ridge and Segamat sections.

6. CONCLUSIONS

a) Turbidities black shale of the Semantan Formation represented the distal part of the submarine fan system and characterized by thin-thick bedded with parallel lamination. In most of the stratigraphic sections, the black shales have upper contact with volcanoclastics and lower with interbedded sandstone and shale, which is further overlain by conglomerate-coarse grained sandstone facies.

b) Based on Rock-Eval pyrolysis, the occurrence of Type–III kerogens is designated in the black shale, which is indicative of organic influx from high terrestrial plants, which is further endorsed by UV-Vis absorption ratios of E2/E4 (A254/A436). This organic matter content is supposed to occur over–matured phase. The binary plot of TOC versus S1 designates organic matter as allochthonous, representing that the source rock itself did not produce the organic matter. Allochthonous nature of organic matter indicates that organic substances transported by turbidity currents from fluvial systems to deep-marine.

c) FTIR spectra show three most abundant spectra from the black shales such as OH functional group stretching, the absorption spectrum of Aromatic C=C stretching, and Aromatic out of plane C–H bending. The dominance of aromatic compounds indicates the possibility of the terrestrial origin of these organic matters.

AKNOWLEDGEMENT

The authors would like to thank Universiti Teknologi Petronas, Malaysia for supporting and funding this research.

REFERENCES

[1] Weimer P. and Pettingill H. S. 2007. Global overview of deep-water exploration and production. In: Nilsen, T. H., Shew, R. D., Steffens, G. S. and Studlick, J. R. J. (eds.) Atlas of Deep outcrops. AAPG Studies in Geology. 56: 7-11.

[2] Metcalfe I. 2013. Gondwana dispersion and Asian accretion: Tectonic and palaeogeographic evolution of eastern Tethys. Journal of Asian Earth Science. 66: 1-33.

[3] Tate R. B., Tan D. N. K. and NG T. F. 2008. Geological Map of Peninsular Malaysia. Scale 1:1 000 000. Geological Society of Malaysia and University of Malaya.

[4] Abdullah N. T. 2009. Mesozoic Stratigraphy. In: Hutchison, C. S. and Tan, D. N. K. (eds.) Geology of Peninsular Malaysia. University of Malaya, Geological Society of Malaysia. 129-131.

[5] Ahmad, J. B. 1976. The geology and mineral resources of the Karak and Temerloh areas, Pahang. Geological Survey of Malaysia, 15: 138.

[6] Metcalfe I. and Chakraborty K. R. 1994. A stratigraphic log of Semantan Formation along part of the Mentakab-Temerloh Bypass, Pahang. Geological Society of Malaysia. 35: 37-46.

[7] Khoo K. K. 1998. Geology and Mineral Resources of the Kuala Pilah Area, Negeri Sembilan. Geological Survey of Malaysia Map Report. 11: 93.

[8] Hutchison C. S. and Tan D. N. K. 2009. Tectonic evolution. In: Hutchison, C. S., Tan, D. N. K., (eds.) Geology of Peninsular Malaysia. University of Malaya/Geological Society of Malaysia, Kuala Lumpur. 309-330.

[9] Mohamed K. R., Joeharry N. A. M., Leman M. S. and Ali C. A. 2016a. The gua musang group: A newly proposed stratigraphic unit for the permo-triassic sequence of northern central belt, peninsular Malaysia. Geological Society of Malaysia Bulletin. 62: 131-142.

[10] Tucker M. E. 2003. Sedimentary rocks in the field, The Geological Field Guide Series. 3rd edition, John Wiley & Sons.

[11] Painter P. C., Snyder R. W., Starsinic M., Coleman M. M., Kuehn D. W. and Davis A 1981.Concerning the application of FT-IR to the study of coal; a critical assessment of band assignments and the application of spectral analysis programs. Applied Spectroscopy. 35(5): 475-485.

[12] Millayanti A., Aprianto A. R., Fauzan R. F. and Anggara M. U. 2019. Evaluation of Organic Matters, Hydrocarbon Potential and Thermal Maturity of Source Rocks Based on Geochemical and Statistical Methods: Case Study Miocene of the Seblat and Lemau Formation, Bengkulu Basin. In: IOP Conference Series: Earth and Environmental Science, IOP Publishing. 12075.

[13] Langford F. F. and Blanc-Valleron M. M. 1990. Interpreting Rock-Eval pyrolysis data using graphs of pyrolizable hydrocarbons vs. total organic carbon (1). American Association Petroleum Geologists Bulletin, 74: 799-804.

[14] Mukhopadhyay P. K., Wade J. A. and Kruge M. A. 1995. Organic facies and maturation of Jurassic/Cretaceous rocks, and possible oil-source rock correlation based on pyrolysis of asphaltenes, Scotian Basin, Canada. Organic Geochemistry. 22: 85-104.

[15] Cunha T. J. F., Novotny E. H., Madari B. E., Martin-Neto L., de O Rezende M. O., Canelas L. P. and de M Benites V. 2009. Spectroscopy characterization of humic acids isolated from Amazonian dark earth soils (Terra Preta de Índio). In: Amazonian Dark Earths: Wim Sombroek's Vision. Springer, 363-372.

[16] Santos L., Pinto A., Filipe O., Cunha Â., Santos E. B. H. and Almeida A. 2016. Insights on the optical properties of estuarine DOM–hydrological and biological Influences. PLoS One, DOI:10.1371/journal.pone.015451.

[17] Hur J., Williams M. A. and Schlautman M. A. 2006. Evaluating spectroscopic and chromatographic techniques to resolve dissolved organic matter via end member mixing analysis. Chemosphere. 63: 387-402.

[18] Battin T. J. 1998. Dissolved organic matter and its optical properties in a blackwater tributary of the upper Orinoco river, Venezuela. Organic Geochemistry. 28: 561-569.

[19] Tipping E., Corbishley H. T., Koprivnjak J. F., Lapworth D. J., Miller M. P., Vincent C. D. and Hamilton-Taylor J. 2009. Quantification of natural DOM from UV absorption at two wavelengths. Environmental Chemistry. 6: 472-476.

[20] Peuravuori J. and Pihlaja K. 1997. Molecular size distribution and spectroscopic properties of aquatic humic substances. Analytical Chimica Acta. 337: 133-149.

[21] Hunt J. F. and Ohno T. 2007. Characterization of fresh and decomposed dissolved organic matter using excitation-emission matrix fluorescence spectroscopy and multiway analysis. Journal of Agriculture Food Chemistry. 55: 2121-2128.

[22] Erlandsson M., Futter M. N., Kothawala D. N. and Köhler S. J. 2012. Variability in spectral absorbance metrics across boreal lake waters. Journal of Environmental Monitoring. 14: 2643-2652.

[23] Mohamed K. R., Joeharry N. A. M., Leman M. S. and Ali C. A. 2016b. The gua musang group: A newly proposed stratigraphic unit for the permo-triassic sequence of northern central belt, peninsular Malaysia. Geol. Soc. Malaysia. 62, 131-142.

[24] Dembicki H. 2016. Practical petroleum geochemistry for exploration and production. Elsevier. 342.